Pertanika J. Sci. & Technol. 31 (6): 3013 - 3038 (2023)

PERTANIKA JOURNALS

SCIENCE & TECHNOLOGY

Journal homepage: http://www.pertanika.upm.edu.my/

Chitosan Dissolution in [BMIM]Cl Ionic Liquid: An Optimisation and Bacterial Ecotoxicity Study

Mok Shue Yee[1], Magaret Sivapragasam[2] and Maisara Shahrom Raja Shahrom[2]*

[1]School of Postgraduate Studies, Research and Internationalisation (SPRINT), Faculty of Integrated Life Sciences, QUEST International University, 30250 Ipoh, Perak, Malaysia
[2]School of Integrated Sciences, Faculty of Integrated Life Sciences, QUEST International University, 30250 Ipoh, Perak, Malaysia

ABSTRACT

Chitosan is formed from chitin deacetylation, but its insolubility remains challenging for industrial applications. An alternative would be employing Ionic Liquids (ILs) as a potential green solvent to dissolve chitosan. Hence, this research aims to study the optimum conditions of chitosan-[BMIM]Cl dissolution using Response Surface Methodology (RSM) and evaluate the ecotoxicity of chitosan-[BMIM]Cl mixture against Gram-positive and Gram-negative bacteria. Chitosan was obtained from heterogenous N-deacetylation of chitin using 50% sodium hydroxide solution at 100°C for 2.5 h. Chitosan dissolution in [BMIM]Cl was optimised using Central Composite Design (CCD) via RSM based on three independent factors: temperature, initial chitosan loading and dissolution time. Ecotoxicity of chitosan-[BMIM]Cl was evaluated using broth microdilution test against *Escherichia coli* and *Staphylococcus aureus*. Chitosan with a degree of deacetylation (DD) of 83.42% was obtained after three successive alkali treatments. Fourier Transform Infrared Spectroscopy (FTIR) revealed the presence of free hydroxyl groups, additional amino groups, and reduced C=O and C-H stretch intensity, indicating successful chitin deacetylation. The regression model for chitosan dissolution in [BMIM]Cl was significant ($p < 0.05$) with a non-significant lack of fit ($p > 0.05$). The optimised conditions to dissolve chitosan in [BMIM]Cl was 130°C, 1 wt. % and 72 h with a mean relative error of 1.78% and RMSE of 5.0496 wt. %. The toxicity of 10 wt. % chitosan-[BMIM]Cl mixture was "relatively harmless" ($EC_{50} > 1000$ mg/L) with an EC_{50} value of 3.1 wt. % for *Escherichia coli* and 3.2 wt. % for *Staphylococcus aureus*.

Keywords: Bacterial ecotoxicity, chitosan, dissolution, ionic liquids, optimisation

ARTICLE INFO

Article history:
Received: 10 November 2022
Accepted: 10 May 2023
Published: 09 October 2023

DOI: https://doi.org/10.47836/pjst.31.6.21

E-mail addresses:
shueyee.mok@qiu.edu.my (Mok Shue Yee)
magaret_62@yahoo.co.uk (Magaret Sivapragasam)
maisarashahrom@hotmail.com (Maisara Shahrom Raja Shahrom)
* Corresponding author

ISSN: 0128-7680
e-ISSN: 2231-8526

INTRODUCTION

The seafood industry generates approximately 10^6 tonnes of seafood waste annually, the major source of chitin extraction, particularly from crustaceans such as shrimp and crab shell residues (Schmitz et al., 2019). Chitin is a natural polysaccharide first discovered in 1811 by Henri Braconnot that can be found abundantly in crustaceans, the exoskeleton of arthropods and the cell walls of fungi and yeast (Rinaudo, 2006).

Chitin is the second most abundant biomass found naturally in the environment after cellulose. Like cellulose, chitin is highly insoluble and has a low chemical reactivity. In recent years, biorefinery has been one of the most important aspects of the circular bioeconomy, referring to an ingenious and efficient route to fully utilise the accessible biomass resources (IEA Bioenergy, 2020) for the following reasons: cost-effectiveness, mitigation of environmental impacts, and optimising the impacts on socio-economic development. Hence, chitin biomass is the perfect candidate due to its high abundance, continuous supply, ease of accessibility, and versatility (Manzanares, 2020). Partial deacetylation of chitin under alkaline conditions produces chitosan, the most important chitin derivative widely used in the industry (Elieh-Ali-Komi & Hamblin, 2016).

Chitosan is a linear polysaccharide comprising monomers of N-acetyl D-glucosamine and D-glucosamine. The properties of chitosan, such as its biodegradability, biocompatibility, toxic-free, film-forming and antibacterial property, encourages the usage of chitosan in various fields such as agricultural (Zhang et al., 2022), biomedical (Zhao et al., 2018), cosmetics (Aranaz et al., 2018), beverages (Liu et al., 2022), water and waste treatment (Morin-Crini et. al., 2019). Chitosan has extensive intermolecular and intramolecular hydrogen bonds that contribute to the poor solubility of chitosan. It is insoluble in neutral or basic solutions but readily dissolved in dilute acidic solutions (Rinaudo, 2006). Chitosan is usually dissolved in 0.1 M acetic acid, but it is also soluble in organic acids such as formic acid, lactic acid, L-ascorbic acid and inorganic acids such as hydrochloric acid and phosphorous acid (Roller & Covill, 1999; Romanazzi et al., 2009). However, the industrial applications of chitosan are still scarce due to its insolubility in most conventional organic solvents. In addition, conventional solvent systems are highly volatile, corrosive, toxic and have limited reusability (Sun, Tian et al., 2014). Therefore, more environmentally friendly solvents to dissolve chitosan is most required.

Ionic liquids (ILs) have been used extensively as an alternative solvent in chemical reactions due to their negligible vapour pressure, greater thermal stability, and highly versatile nature (Claros et al., 2010). The physicochemical properties of ILs can be altered by selecting an appropriate anion or cation of ILs, making them useful in a wider range of applications (Thomas & Marvey, 2016). Previous studies have explored the usage of ILs in the context of biomass processing, such as the fractionation of softwood and wheat straw into sugars such as glucose and pentose, respectively, as well as facilitating the separation

between lignin and cellulose (da Costa Lopes et al., 2018; Gschwend et al., 2019). ILs had been shown capable of dissolving natural polymers such as cellulose (Swatloski et al., 2002; Wu et al., 2004), carbohydrates (Forsyth et al., 2002), chitin (Wang et al., 2010) and chitosan (Zhuang et al., 2020) because ILs have outstanding solvation potential and the role of anion within ILs to disrupt extensive hydrogen bonds within these macromolecules (Rosatella et al., 2009; Zakrzewska et al., 2010).

ILs are widely recognised as green solvents due to their insignificant vapour pressure. However, being non-volatile does not mean that ILs are toxic-free (Lei et al., 2017). Therefore, the ecotoxicity of ILs has been assessed by several researchers (Egorova & Ananikov, 2014; Bubalo et al., 2017; Sivapragasam et al., 2019; Sivapragasam et al., 2020). ILs are very soluble in water, readily dissociate into their respective ions and migrate easily into an aqueous system. Accumulation in water systems may directly affect aquatic organisms and indirectly affect higher organisms, such as humans, upon consumption of contaminated fish. Therefore, it is important to evaluate the ecotoxicity of ILs to determine the value of EC_{50}, defined as the effective concentration that inhibits the growth of organisms by 50%, which can be achieved using microorganisms due to shorter generation time, faster growth rate and easily available (Sivapragasam et al., 2020).

The present study used RSM to study the optimisation of chitosan dissolution in ILs, [BMIM]Cl. The optimised chitosan dissolution was subjected to ecotoxicity assessment to establish the toxicity of the chitosan-ILs mixture on Gram-positive bacteria and Gram-negative bacteria, *Staphylococcus aureus* and *Escherichia coli*. From this research, the optimised conditions to dissolve chitosan in [BMIM]Cl was established based on three factors (temperature, initial chitosan loading and dissolution time) and the ecotoxicity of chitosan-[BMIM][Cl] was determined.

The impact of this research helps realise a few of the Sustainable Development Goals (SDGs) initiated by the United Nations, which are the sixth, fourteenth and fifteenth goals, which are Clean Water and Sanitation, Life Below Water and Life on Land, respectively. Complete biomass dissolution is desirable for the valorisation and fractionation of biomass macromolecules into their respective constituents, thus enhancing the competency and economic viability of biorefinery products (Rodríguez, 2021), such as the dissolution of chitosan in ILs for various applications such as glucose biosensor, CO_2/N_2 separation and the adsorption of malachite green dye from aqueous solutions (Zhang et al., 2013; Santos et al., 2016; Naseeruteen et al., 2018).

MATERIALS AND METHODS

Coarse chitin flakes from shrimp shells, practical grade (≥ 95% acetylated) and pure silicone oil (cSt 1000) were purchased from Sigma-Aldrich (Missouri, United States) and used without further purification. Sodium hydroxide (NaOH) pellets, A.R grade (≥ 96%) was

purchased from Bendosen (Selangor, Malaysia). Dimethyl sulfoxide (DMSO), A.R grade (≥ 99.8%), was purchased from Systerm Chemicals (Selangor, Malaysia). Acetone, A.R grade (≥ 99.7%), was purchased from QReC (Selangor, Malaysia). Mueller-Hinton broth and potassium bromide KBr powder were purchased from Sisco Research Laboratories Pvt. Ltd (Mumbai, India) and PIKE Technologies (Wisconsin, United States), respectively. KBr powder was dried at 100°C for 2 h before its use. 1-butyl-3-methylimidazolium chloride, [BMIM]Cl (0.85% H_2O) was obtained from the Centre of Research in Ionic Liquids, Universiti Teknologi PETRONAS, Malaysia, as a gift.

Deacetylation of Chitin

Deacetylation of chitin was performed using the protocol described by El Knidri et al. (2016). Chitosan was obtained by deacetylating chitin flakes from shrimp shells with 50% (w/v) concentrated NaOH at 100°C for 2 h 30 min, using a ratio of chitin to NaOH of 1:20 (g:mL). After the reaction, the product was washed with distilled water until the pH of chitosan became neutral. Partial deacetylation of chitosan was repeated another two times to obtain chitosan with a higher deacetylation degree (DD). Chitosan was dried in an oven at 80°C for 24 h after repeated alkali treatments.

Characterisation of Chitosan Using Fourier Transform Infrared (FTIR) Spectroscopy

Chitin and chitosan were characterised using FTIR (Bruker Alpha II, Massachusetts, United States) in the 4000 to 650 cm^{-1} range using the KBr pellet method (Poerio et al., 2021). For each sample, 16 scans were performed with a resolution of 4 cm^{-1}. The DD of chitosan was calculated using FTIR using the absorption band at 1320 and 1420 cm^{-1}, corresponding to a characteristic band of acetylated amine or amide and a reference band, respectively (Brugnerotto et al., 2021). The deacetylation degree, DD % of chitosan, was calculated using Equation 1, where A_{1320} and A_{1420} are the absorption bands at 1320 cm^{-1} and 1420 $cm^{-1,}$ respectively.

$$DD\%\ (\%) = 100\% - \frac{\frac{A_{1320}}{A_{1420}} - 0.3822}{0.03133} \quad (1)$$

Optimisation of Dissolution Parameters Using Response Surface Methodology (RSM)

Parameters for chitosan dissolution in [BMIM]Cl were optimised via RSM using Design Expert version 12.0.3.0 (Stat-Ease, Minnesota, United States). This study explored the effects of three independent variables towards chitosan dissolution in [BMIM]Cl using the CCD model. The three independent variables were temperature (X_1, 90°C to 130°C), initial chitosan loading (X_2, 1 wt. % to 7 wt. %) and dissolution time (X_3, 24 h to 72 h).

The highest and lowest values for each variable were selected based on previous studies by Sun, Xue et al. (2014), Islam et al. (2015) and Xu et al. (2016). The dependent variable was dissolution percentage (Y, wt. %). A total of 20 randomly suggested experiments generated by the CCD model were performed. Table 1 shows the level of parameters of chitosan dissolution in [BMIM]Cl. The relative error calculation for the RSM model was carried out by conducting the optimised conditions in triplicates.

Table 1
Level of parameters for chitosan dissolution in [BMIM]Cl using CCD model

Variables	Coding	Unit	Coded Levels of Experimental Factors		
			-1	0	1
Temperature	X_1	°C	90	110	130
Initial chitosan loading	X_2	wt. %	1	4	7
Time of dissolution	X_3	h	24	48	72

Dissolution of Chitosan in ILs, [BMIM]Cl

The dissolution of chitosan in [BMIM]Cl was performed according to the methodology outlined by Sun et al. (2009) using parameters suggested by RSM. Approximately 2 g of [BMIM]Cl was added to a universal bottle and immersed in an oil bath with a temperature instability of ±2°C. Prior to dissolution, chitosan was dried in an oven at 80°C for 24 h to remove moisture. An appropriate amount of chitosan (wt. %) was added and stirred continuously at 500 rpm, and the RSM model suggested the temperature and dissolution time.

Undissolved chitosan was removed according to procedures described by Sun et al. (2009). Briefly, 10 mL of DMSO was added to the universal bottle containing undissolved precipitate and chitosan-ILs solution. The solution was vortexed vigorously and centrifuged at 100 g for 10 min. The supernatant was kept in a separate Falcon tube for regeneration of dissolved chitosan. The precipitate was washed again with DMSO 3 times and subsequently washed with 20 mL of distilled water for another 3 times. The precipitate was dried in an oven at 60°C for 24 h and weighed after drying. Equation 2 was used to compute the dissolution percentage of chitosan, where w_o and w_p are the initial weight of chitosan and undissolved chitosan, respectively.

$$Dissolution\ \%\ (wt.\%) = \frac{[W_o - W_p]}{W_o} \times 100 \quad (2)$$

Regeneration of Dissolved Chitosan

Chitosan dissolved in [BMIM]Cl was regenerated using procedures described in Rahim et al. (2018). The chitosan-ILs solution was mixed with 15 mL of acetone (9:1) and vortexed vigorously. The mixture was centrifuged at 4000 rpm for 15 min, and the supernatant was

discarded. The pellet formed was washed again with 15 mL of acetone solution (9:1), vortexed and centrifuged at 4000 rpm for 15 min. The precipitate was washed another 3 times and left to air dry in a fume hood to remove residual acetone solution from the regenerated chitosan. Regenerated chitosan was dried in an oven at 60°C for 24 h.

Characterisation of Chitosan-IL Using Fourier Transform Infrared (FTIR) Spectroscopy

Chitosan (pure) and pre-treated chitosan (after dissolution in ILs) were analysed using FTIR Spectroscopy (Bruker Alpha II, Massachusetts, United States) to check any chemical changes that occurred during the dissolution. Chitosan-ILs solution was analysed to see the incorporation of chemical compounds of ILs and chitosan. FTIR spectra were measured in the 4000-650 cm^{-1} range using the KBr pellet method adapted from Poerio et al. (2021) with some modifications. Sample and KBr were mixed in a ratio of 1:100 and placed into a pellet die to form a transparent pellet. For each sample, 16 scans were taken with a resolution of 4 cm^{-1}.

Broth Microdilution Method

Ecotoxicity of the chitosan-ILs mixture was assessed using broth microdilution method according to standard procedure CLSI-M07-A9, 2008, developed by Clinical and Laboratory Standard Institute (CLSI), USA. Chitosan-ILs solution was diluted using two-fold serial dilution and added to each 96-well plate. Two-fold chitosan-ILs solutions were added to each well from 100,000 ppm (10 wt. %) to 200 ppm (0.020 wt. %). Bacterial suspensions of *Staphylococcus aureus* ATCC 12600 and *Escherichia coli* ATCC 8739 were prepared by transferring a loopful of colonies from a 24-hour bacteria culture to Mueller-Hinton broth. About 100 µL of *Staphylococcus aureus* and *Escherichia coli* dilutions were added into each well containing 100 µL of chitosan-ILs mixture in a separate microdilution plate. About 100 µL of bacteria suspension was used as blank and dispensed into the well A1. Microdilution plates were incubated at 37°C for 24 h, and the absorbance value of each well was determined using a microplate reader (CYBERLAB™ Cyber ELISA-R01, Millbury, United States) at a wavelength of 550 nm. Minimum inhibitory concentration (MIC) and EC_{50} values of chitosan-ILs solution were determined by plotting the absorbance values in a graph generated by Prism version 9.0.0 (GraphPad Software, San Diego, California).

RESULTS AND DISCUSSIONS

Deacetylation of Chitin into Chitosan

Alkaline deacetylation of chitin into chitosan was carried out using 50% NaOH at 100°C for 2.5 h for three successive alkali treatments. Deacetylation of chitin was represented by Equation 3, where the acetamide group in chitin underwent hydrolysis in the presence

of strong NaOH and elevated temperature to form an acetyl group and a reactive amino group, the key functional group that differentiates chitin from chitosan (Fatima, 2020).

$$CH_3CONH_2 \xrightarrow{\text{Deacetylation}} NH_2 + CH_3CO \quad (3)$$

Figure 1 shows chitin flakes before deacetylation and chitosan obtained after partial deacetylation. Chitin flakes before deacetylation were larger (0.4–1.0 cm) and yellowish. Chitosan obtained after three successive alkali treatments was smaller (0.1–0.3 cm) and white, which is in accordance with Kusuma et al. (2015) that chitosan produced has a more pronounced white colour than chitin. Chitosan produced was also odourless and present in the crystalline flakes, which was also observed by Ahing and Wid (2016).

Tamzi et al. (2020) corroborate findings where chitin and chitosan prepared from shrimp (*Panaeusmonodon monodon*), and crab shells (*Scylla serrata*) were yellowish-white and off-white, respectively—the change in colour from yellowish-white to brighter was related to removing acetyl groups during chitin deacetylation.

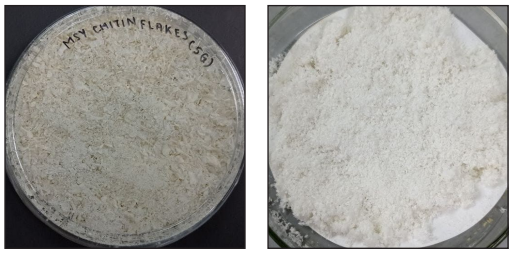

(a) (b)

Figure 1. (a) Chitin flakes before deacetylation; (b) and chitosan obtained after three successive alkali treatments

Characterisation of Chitin and Chitosan Using FTIR. The structure of chitin and chitosan was analysed by identifying the functional groups and bonds obtained from the spectrum generated using FTIR. The functional groups present in chitin are hydroxyl group (-OH), acetamide group (-CH_3CONH) and an ether group (C-O-C) between neighbouring glucosamine residues (Elieh-Ali-Komi & Hamblin, 2016). Figure 2 shows the transmittance spectrum of chitin. A strong, broad peak at 3444 cm^{-1} represented the O-H stretch of chitin, indicating the presence of a hydroxyl group in the structure of chitin, which was also observed by Puspawati and Simpen (2010). The sharp peak at 3106 cm^{-1} was attributed to the N-H stretch. Three peaks recorded at 2961, 2932, and 2891 cm^{-1} were due to sp^3 C-H stretch, previously reported by Kusuma et al. (2015) and Matute et al. (2013). The peak at 1655 cm^{-1} overlapped the C=O stretch and N-H bend, the characteristic band of amide I (Rumengan et. al., 2014). The peak at 1560 cm^{-1} was due to N-H in-plane bend and C-N stretch, a characteristic band of amide II in secondary amide. The 1280 to 1070 cm^{-1} peaks were due to C-O-C stretch (Puspawati & Simpen, 2010; Akakuru et al., 2018).

The functional groups that were present in partially deacetylated chitosan are hydroxyl group (-OH), acetamide group (-CH_3CONH), amino group (-NH_2) and ether group (C-O-C) between neighbouring glucosamine residues (Akakuru et al., 2018). Figure 3 shows the

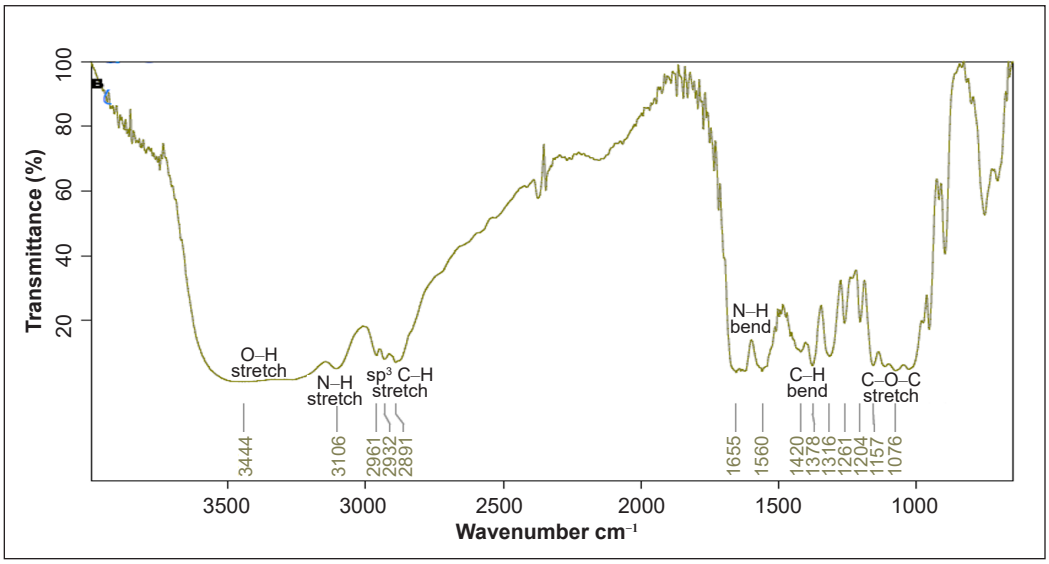

Figure 2. FTIR transmittance spectrum generated by chitin

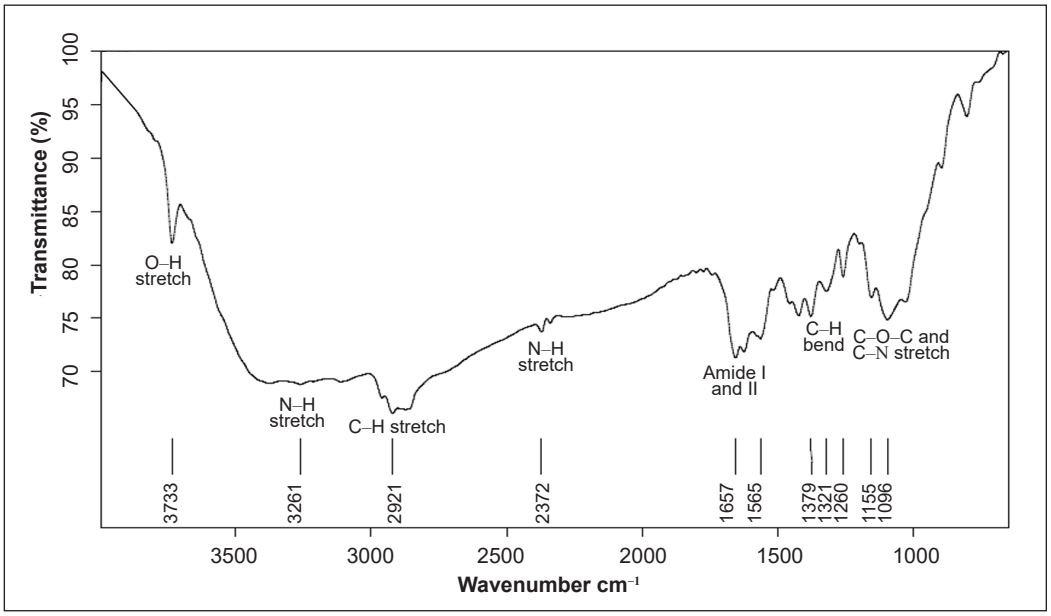

Figure 3. FTIR transmittance spectrum generated by chitosan

transmittance spectrum of chitosan obtained from partial deacetylation of chitin. The sharp peak at 3733 cm^{-1} was due to the stretch of the free OH group. The peak at 3261 and 2372 cm^{-1} was due to the N-H stretch, as Matute et al. (2013) reported. The peak at 2921 cm^{-1} was attributed to C-H stretch in the aliphatic compound, particularly symmetric CH_3 and asymmetric CH_2 (Palpandi et al., 2009). The peak at 1657 and 1565 cm^{-1} was caused by

the absorption of amide I and II bands, respectively. Amide I band still appears in the FTIR spectrum because chitin was not completely deacetylated to form chitosan with a DD of 100 %. Three peaks recorded at 1260, 1155 and 1096 cm^{-1} were due to C-O and C-N stretch (Kusuma et al., 2015).

Several peaks in the FTIR spectrum of chitin and chitosan can be used to distinguish between the functional groups in chitin and chitosan. The hydroxyl group in chitosan is a free hydroxyl group attributed by a sharp peak at 3733 $cm^{-1,}$ while the hydroxyl group in chitin is bonded to hydrogen, attributed by the peak of 3444 cm^{-1}. One peak was observed at 3106 cm^{-1} due to N-H stretch in chitin, but there were two peaks at 3261 and 2372 cm^{-1} caused by N-H stretch in chitosan due to additional amino groups. In addition, C-N stretch was also observed in the range of 1250 to 1020 cm^{-1} in the FTIR spectrum of chitosan but absent in the chitin spectrum. Lastly, the absorption of infrared radiation by C-H stretch and amide I band in chitin was greater than that in chitosan as there were more acetyl ($-C_2H_3O$) and acetamide groups respectively in the crystalline chain of chitin. Larger absorption at 2885 cm^{-1} in chitin was due to higher C-H bonds (Rumenagan et al., 2014). In our study, the peak at 2891 cm^{-1} attributed to C-H stretch in chitin disappeared in the FTIR spectrum of chitosan after partial deacetylation of chitin. It correlated well with the findings from Ahyat et al. (2017), indicating a successful elimination of acetyl group in the chemical structure of chitin during deacetylation. Dennis et al. (2016) reported reduced peaks due to the loss of acetyl groups in their FTIR spectrum- which correlates well with this study.

Determination of Degree of Deacetylation of Chitosan Using FTIR. DD was obtained from FTIR using the A_{1320}/A_{1420} tallies ratio with the degree of deacetylation obtained using ^{1}H and ^{13}C NMR. The absorption band at 1320 and 1420 cm^{-1} was unaffected by the humidity of the sample (Czechowska-Biskup et al., 2012). Figure 4 shows the absorbance spectrum of chitosan obtained from the heterogenous N-deacetylation of chitin flakes. Based on Figure 4, the absorbance at 1320 cm^{-1} and 1420 cm^{-1} was 0.11 and 0.122, respectively.

$$DD\%\ (\%) = 100\% - \frac{\frac{A_{1320}}{A_{1420}} - 0.3822}{0.03133} \quad (4)$$

$$DD\% = 100\% - \frac{\frac{0.11}{0.122} - 0.3822}{0.03133} = 83.42\% \quad (5)$$

Based on Equation 4, proposed by Brugnerotto et al. (2001), the DD of chitosan from this study was 83.42%, as shown in Equation 5. With a DD of 83.42%, it has 83.42% of the amino group and 16.58% of the acetyl group in its chain.

Based on the FTIR spectrums obtained from both chitin and chitosan samples, it can be confirmed that chitosan was successfully synthesised (DD ≥ 60%) from heterogenous

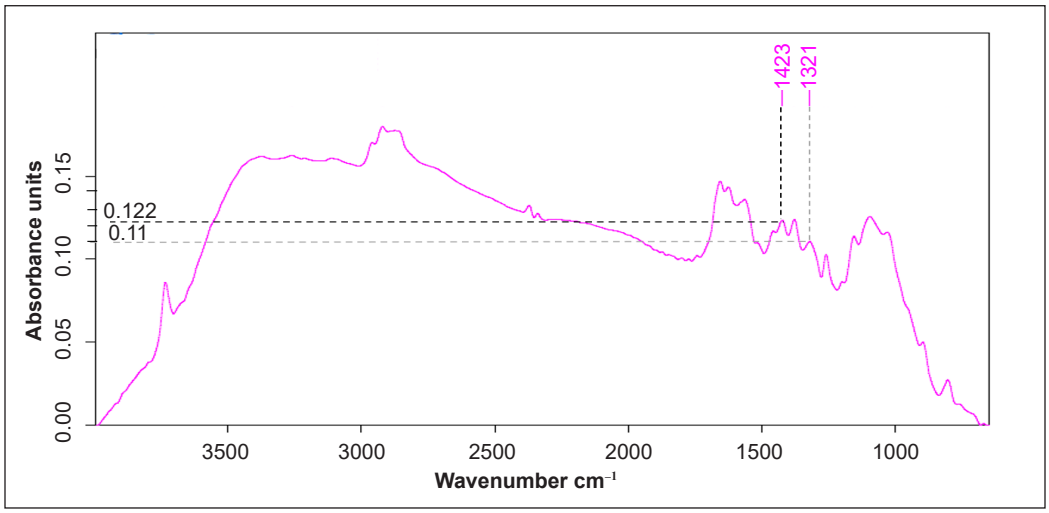

Figure 4. FTIR absorbance spectrum generated by chitosan

N-deacetylation of chitin flakes from shrimp shell using 50% concentrated NaOH solution. Synthesised chitosan was used in RSM to optimise the dissolution of chitosan in [BMIM]Cl based on three independent factors: temperature, initial chitosan loading and dissolution time.

Optimisation of Chitosan Dissolution Using Response Surface Methodology (RSM)

RSM was applied to optimise the dissolution of chitosan in [BMIM]Cl. This study's experiment design was CCD based on three independent factors: temperature, initial chitosan loading and dissolution time. The suggested experimental runs generated by the RSM model and experimental results are shown in Table 2. The highest dissolution percentage was obtained in standard run 6 with a value of 95 wt. % (X_1 = 130°C, X_2 = 1 wt. %, X_3 = 72 h), followed by standard run 2 with a dissolution percentage of 94.5% (X_1 = 130°C, X_2 = 1 wt. %, X_3 = 24 h). The lowest dissolution percentage of 17.79 wt. % was obtained in standard run 3 (X_1 = 90°C, X_2 = 7 wt. %, X_3 = 24 h).

Design-Expert version 12.0.3.0 was employed to study the experimental data's regression analysis and plot the response surface curves. The statistical parameters were evaluated using analysis of variance (ANOVA), and the fitness of the regression model was evaluated using a lack of fit test, as demonstrated in Table 3. A model will fit the experimental data well if the regression model is significant and the lack of fit test is not significant with a 95% confidence level.

According to Table 3, the regression model for the dissolution percentage of chitosan was significant, with a F-value of 99.24 and a p-value < 0.0001. The model F-value of 99.24 indicated that there was only a 0.01% chance that the model F-value could occur due to noise. All the independent variables tested in this study were significant, with p-value < 0.05. The

lack of fit test was insignificant, with an F-value of 2.11 and a p-value of 0.2114, respectively. Significant regression and non-significant lack of fit test indicated that the experimental data fits the data well and can be used to optimise the dissolution of chitosan in [BMIM]Cl. The experimental data was fitted into a linear model, suggested by the RSM software. It showed that there were no interactions between the independent variables.

Table 2
Experimental design for dissolution of chitosan in [BMIM]Cl generated by RSM

Standard	Run	Factor 1 X_1: Temperature (°C)	Factor 2 X_2: Initial Chitosan Loading (wt. %)	Factor 3 X_3: Dissolution Time (h)	Response Dissolution Percentage (wt. %)
1	20	90	1	24	71.500
2	7	130	1	24	94.500
3	14	90	7	24	17.790
4	5	130	7	24	20.640
5	18	90	1	72	89.500
6	15	130	1	72	95.000
7	9	90	7	72	27.570
8	11	130	7	72	43.210
9	8	90	4	48	50.500
10	2	130	4	48	49.750
11	4	110	1	48	83.000
12	1	110	7	48	30.070
13	16	110	4	24	45.000
14	12	110	4	72	66.250
15	13	110	4	48	59.320
16	6	110	4	48	60.625
17	19	110	4	48	55.750
18	3	110	4	48	67.250
19	17	110	4	48	55.750
20	10	110	4	48	60.250

Table 3
Analysis of variance (ANOVA) for dissolution percentage

Source	Sum of Squares	df	Mean Square	F-value	p-value	Remarks
Model	9390.20	3	3130.07	99.24	< 0.0001	Significant
X_1: Temperature	213.81	1	213.81	6.78	0.0192	
X_2: Initial Chitosan Loading	8656.54	1	8656.54	274.45	< 0.0001	
X_3: Dissolution Time	519.84	1	519.84	16.48	0.0009	
Residual	504.67	16	31.54			
Lack of Fit	415.25	11	37.75	2.11	0.2114	Not significant
Pure Error	89.42	5	17.88			
Cor Total	9894.87	19				

Table 4 shows the fit statistics of the regression model for the dissolution percentage of chitosan in [BMIM]Cl. The adequacy of the model was determined using the coefficient determination value, R^2. The R^2 value of the regression model was 0.9490, suggesting a good correlation between experimental and predicted values. Adjusted R^2 measures the variation of the mean obtained from the model. Predicted R^2 refers to the R^2 value estimated from the regression model (Behera et al., 2018). The adjusted and predicted R^2 value was 0.9394 and 0.9155, respectively, with a difference of only 0.0239, indicating that the R^2 predicted from the regression model agreed reasonably with the adjusted R^2 value. The actual and predicted values for dissolution percentage are as per Figure 5, which showed a reasonably good response estimate and indicated the model's good performance.

Signal to noise ratio was calculated by determining the value of adequate precision. Adequate precision greater than 4 is desirable and can be utilised to navigate design space. The adequate precision obtained from this regression model is 32.8517, greater than 4. Therefore, the regression model can predict the dissolution percentage of chitosan in [BMIM]Cl.

Figures 6, 7 and 8 show the contour plots for dissolution percentage at 24, 48 and 72 h dissolution times, respectively. From Figures 6, 7 and 8, the dissolution of chitosan increases with temperature and dissolution time but decreases with initial chitosan loading.

Table 4
Fit statistics for dissolution percentage

Standard Deviation	5.62	R^2	0.9490
Mean	57.16	**Adjusted R^2**	0.9394
C.V. %	9.83	**Predicted R^2**	0.9155
		Adequate Precision	32.8517

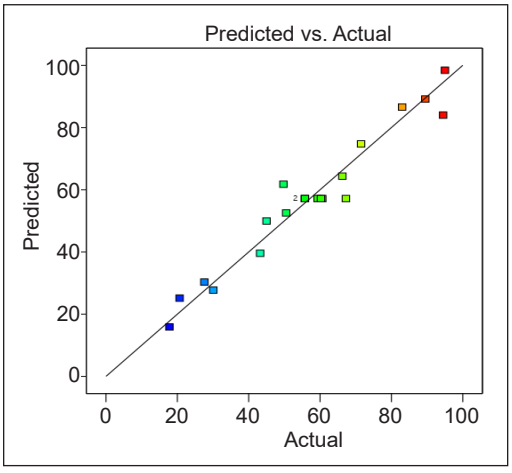

Figure 5. Actual and predicted values for dissolution percentage

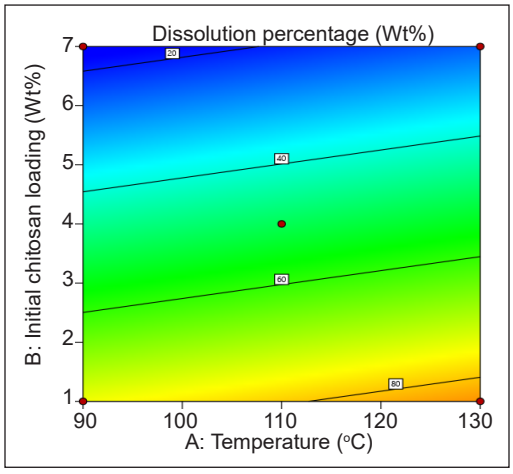

Figure 6. Contour plots at a dissolution time of 24 h

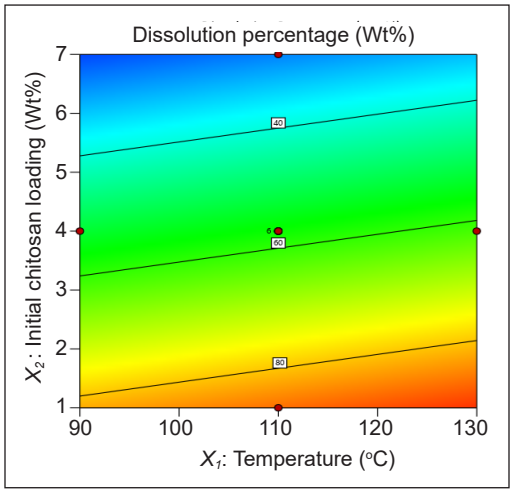

Figure 7. Contour plots at a dissolution time of 48 h

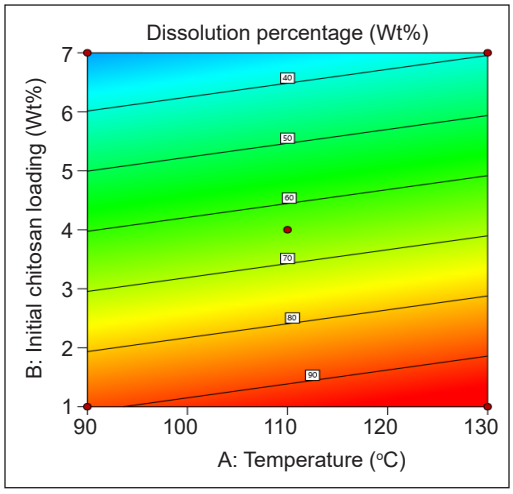

Figure 8. Contour plots at a dissolution time of 72 h

Effect of Temperature on Dissolution Percentage of Chitosan in [BMIM]Cl. Chitosan dissolution in [BMIM]Cl increases with 90 to 130°C temperature was relatively the least important among the tested variables that affected the dissolution percentage of chitosan, with the smallest F-value of 6.78. Increasing the temperature decreased the viscosity of [BMIM]Cl and accelerated the swelling of chitosan and mixing of chitosan-[BMIM]Cl (Tan & Lee, 2012). The increase in temperature also caused hydrogen bonds within chitosan to be partially disrupted. The effect of temperature on the dissolution of chitosan in [BMIM][Ac] has been studied by Chen et al. (2011), who observed that chitosan solubility increased with increasing temperatures. Chitosan solubility in [BMIM][Ac] at 150°C (14.4 wt. %) was enhanced by 9 times that at 70°C (1.6 wt. %). Enhanced chitosan dissolution showed that a temperature rise had partially disrupted some of the hydrogen bonds. Sun, Tian et al. (2014) reported that relatively high temperatures improved chitosan dissolution by accelerating the evaporation of remaining water from the ILs, which acted as an anti-solvent during the solubilisation reaction. They also observed that a temperature increment by 10°C decreased the viscosity of ILs by half, with a greater dissolving ability of chitosan in ILs.

Effect of Initial Chitosan Loading on Dissolution Percentage of Chitosan in [BMIM]Cl. Initial chitosan loading is inversely proportional to the dissolution of chitosan in [BMIM]Cl. Initial chitosan loading was the most important variable that affected the dissolution percentage of chitosan due to a high F-value of 274.45. The ratio of biopolymer to ILs strongly impacted the dissolution reaction. At lower chitosan loading, chitosan was more dispersed, facilitating the diffusion of [BMIM]Cl into the crystalline region of chitosan, subsequently increasing the dissolution rate and dissolution percentage due to enhanced frequency of effective collisions between chitosan and ILs (Chowdhury et al., 2014). Similar

findings had been reported by Sun et al. (2009) by dissolving various amounts of wood in [EMIM][Ac] from 4 wt. % to 10 wt. %. They observed that as the initial wood loading increases, a lower percentage of wood was dissolved in the ILs from 99.5% in 4 wt. % of the wood in [EMIM][Ac] to 40% in 10 wt. % of wood in [EMIM][Ac].

Effect of Dissolution Time on Dissolution Percentage of Chitosan in [BMIM]Cl. As the dissolution time increases, the dissolution percentage of chitosan increases, represented by an upward slope. Dissolution time was the second most important variable after initial chitosan loading, with a F-value of 16.48. Longer dissolution time, they encouraged the diffusion of ILs into the pores of the biomass matrix, improving the dissolution of chitosan in [BMIM]Cl (Ma et al., 2019). Wang et al. (2011) reported the enhancement in the rate of dissolution and regeneration of wood samples in [AMIM]Cl with the increase in reaction time. Pine wood's dissolution and regeneration rates increased from 19% to 26% and 9% to 19 %, respectively, when dissolution time was prolonged from 6 h to 24 h.

Optimisation of Chitosan Dissolution in [BMIM][Cl]. Optimisation of chitosan dissolution was performed via numerical optimisation in Design-Expert software. The final equation in terms of actual factors for dissolution percentage (Y, wt. %) was shown in Equation 6, where X_1, X_2 and X_3 refer to temperature (°C), initial chitosan loading (wt. %) and dissolution time (h), respectively.

$$\text{Dissolution Percentage } (Y, \text{ wt. \%}) = 56.53858+0.2312X_1 - 9.80733X_2+0.300417X_3 \quad (6)$$

To find the best conditions to dissolve chitosan in [BMIM]Cl, all three independent variables, temperature (X_1, °C), initial chitosan loading (X_2, wt. %) and dissolution time (X_3, h), were set within the range. The response variable, dissolution percentage (Y, wt. %), was set at maximum values. Out of 100 solutions suggested by RSM, solution 1 (X_1 = 130°C, X_2 = 1 wt. % and X_3 = 72 h) was chosen due to the highest dissolution percentage of 98.417 wt. % with desirability of 1.000.

The regression model for the dissolution percentage of chitosan was verified by calculating the relative error and root mean square error (RMSE). The relative error of the regression model for dissolution percentage was calculated by carrying out the optimised solution in triplicates and computed using Equation 7.

$$Relative\ error\ (\%) = \frac{Predicted\ value\ -\ Experimental\ value}{Prdicted\ value} \times 100\ \% \quad (7)$$

The relative error of the three runs was shown in Table 5 and was in the range of 0.42 to 3.47%. The mean of relative error for the regression model was 1.78%, indicating

Table 5
Relative error for dissolution percentage

Independent Variables			Dissolution Percentage (wt. %)		Relative Error (%)
X_1 (°C)	X_2 (wt. %)	X_3 (h)	**Predicted**	**Experimental**	
130	1	72	98.417	98	0.42
130	1	72	98.417	97	1.44
130	1	72	98.417	95	3.47

that the values of the dissolution percentage of chitosan predicted were close to that of chitosan obtained experimentally. It validates a good correlation between the predicted and experimental values.

Root mean square error (RMSE) is a commonly used performance metric for evaluating regression models that measure the average difference between the predicted and actual values of the dependent variable (Ali & Abustan, 2014), which can be calculated using Equation 8.

$$RMSE = \sqrt{\frac{(Predicted\ value\ -\ actual\ value)^2}{N}} \tag{8}$$

Table 6 compares predicted and actual values of the dissolution percentage of chitosan in [BMIM]Cl, along with the sum of squares of the residuals.

$$RMSE = \sqrt{\frac{509.9734}{20}} = 5.0496\ wt.\% \tag{9}$$

In the regression model of chitosan dissolution in [BMIM]Cl, the RMSE value obtained is 5.0496 wt. % (Equation 9) suggests that there was approximately a 5 wt. % variation between the predicted values by the regression model and the observed experimental values obtained during the optimisation of chitosan dissolution in [BMIM]Cl.

Although the optimisation of chitosan dissolution in ILs has yet to be reported, numerous studies have attempted to dissolve chitosan in different ILs. [BMIM]Cl was first used to dissolve chitosan with an initial chitosan loading of 10 wt. % by Xie et al. (2006) at 110°C for 5 h in an oil bath in an inert N_2 atmosphere. Meanwhile, more ILs such as [AMIM]Cl, [BMIM]Cl, and [BMIM][Ac] were used to dissolve chitosan with an initial chitosan loading of 8, 10, and 12 wt. %, respectively, at the same temperature and dissolution time (Wu et al., 2008). In our study, we attempted to dissolve chitosan with an initial loading of 4 wt. % at 110°C under continuous stirring in an oil bath in a normal atmosphere for 24 and 72 h, respectively, with an efficiency of 45 and 66.25%.

Table 6
Predicted and actual values of the dissolution percentage of chitosan in [BMIM]Cl

Standard Order	Run Order	Predicted Value (wt. %)	Actual Value (wt. %)	Residual (wt. %)	Square of Residuals (wt. %)
1	20	74.39	71.50	-2.8900	8.3521
2	7	84.49	94.50	10.0100	100.2001
3	14	14.71	13.55	-1.1600	1.3456
4	5	24.81	20.64	-4.1700	17.3889
5	18	88.52	89.50	0.9832	0.9667
6	15	98.62	95.00	-3.6200	13.1044
7	9	28.83	27.57	-1.2600	1.5876
8	11	38.94	43.25	4.3100	18.5761
9	8	51.61	50.50	-1.1100	1.2321
10	2	61.72	49.75	-11.9700	143.2809
11	4	86.51	83.00	-3.5100	12.3201
12	1	26.82	30.07	3.2500	10.5625
13	16	49.60	45.00	-4.6000	21.16
14	12	63.73	60.50	-3.2300	10.4329
15	13	56.66	59.32	2.6600	7.0756
16	6	56.66	60.63	3.9600	15.6816
17	19	56.66	55.75	-0.9138	0.8350
18	3	56.66	67.25	10.5900	112.1481
19	17	56.66	55.75	-0.9138	0.8350
20	10	56.66	60.25	3.5900	12.8881
					Σ = 509.9732

FTIR of Regenerated Chitosan. Untreated chitosan and chitosan regenerated from optimised solution (X_1 = 130°C, X_2 = 1 wt. % and X_3 = 72 h) were characterised using FTIR to analyse for chemical changes that occurred during the dissolution of chitosan in [BMIM]Cl as illustrated in Figure 9.

No observable chemical changes occurred between chitosan before and after dissolution in [BMIM]Cl, as all the spectra depicted in Figure 9 were similar. The only difference in chitosan after regeneration was the disappearance of free hydroxyl groups in chitosan at 3733 cm^{-1} after dissolution in ILs. However, the O-H stretch can be observed at 3443 cm^{-1} of the regenerated chitosan. The spectra for the regenerated chitosan showed more distinct functional groups, such as peaks representing the N-H stretch and amide II band at 3108 and 1561 cm^{-1}. It showed that the dissolution of chitosan in [BMIM]Cl aids in obtaining chitosan of higher purity and enhances the deacetylation process. It also has been noticed in the case of Islam et. al. (2015), where the regenerated chitosan produced clearer and sharper peaks at 3359 cm^{-1} and in 1030-1155 cm^{-1}- indicating enhanced O-H and N-H stretch and C-O stretch, respectively. Shifts in O-H and N-H stretch in regenerated chitosan also indicated an enhancement of hydrogen bonding (Qi et al., 2004).

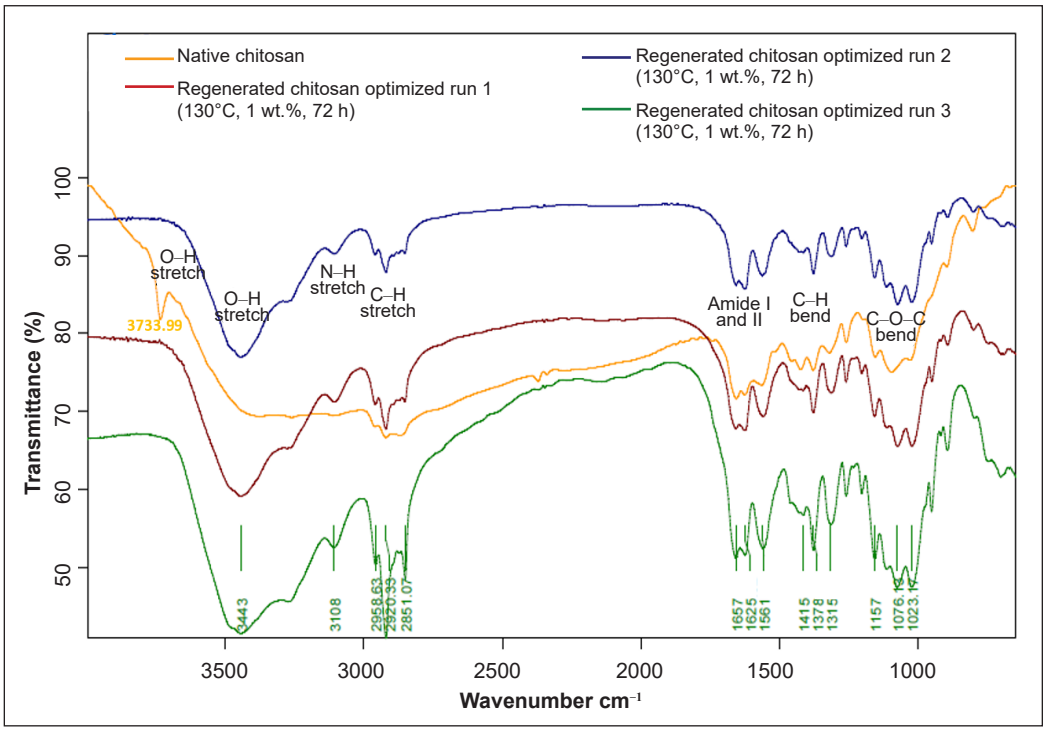

Figure 9. FTIR of chitosan and regenerated chitosan obtained from optimised solution

Due to the similarity between the FTIR spectra of native and regenerated chitosan, results show no chemical reaction between chitosan and [BMIM]Cl during dissolution. In addition, there was no absorption peak observed at 1520 cm^{-1}, indicating the formation of ammonium salt. Therefore, the main chitosan chain was not disrupted after dissolution in [BMIM]Cl as the direct solvent to solubilise chitosan in ILs. Similar results were also reported by Chen et al. (2011), who attempted to study the dissolution of chitosan in [BMIM][Ac].

The ability of ILs to dissolve chitosan is associated with the ability of ILs to accept hydrogen atoms from chitosan to form H-bonds with the anion (Zhang et al., 2005). Yang et al. (2016) stated that the anion of ILs, Cl^- interacts with hydrogen atoms in both the hydroxyl and amino groups, while the cation of ILs, $[BMIM]^+$, interacts with oxygen atoms in hydroxyl and nitrogen atoms. Besides H-bond, intermolecular forces such as ion-induced dipole forces were also observed between the physical interaction of [BMIM]Cl and chitosan. Ion-induced dipole forces occurred when the presence of an ion, $[BMIM]^+$ or Cl^- distorted the electron distribution of a non-polar molecule or atom such as oxygen or hydrogen atom found in hydroxyl and nitrogen atom in the amino group, inducing the formation of a dipole. It was seen by the free hydroxyl group observed at 3733 cm^{-1} in native chitosan but shifted to 3443 cm^{-1} in all the regenerated chitosan, demonstrating the interaction between the cations and anions of ILs with chitosan.

Ecotoxicity of Chitosan-[BMIM]Cl Solution

The ecotoxicity of the chitosan-[BMIM]Cl mixture was assessed against two bacteria species, *Escherichia coli* (Gram-negative) and *Staphylococcus aureus* (Gram-positive), using broth microdilution assay. MIC values were determined to obtain the range (upper and lower limit) of EC_{50} values, which refers to the concentration of chitosan-[BMIM]Cl that inhibits 50% of the bacteria growth. The EC_{50} dose-response curve of chitosan-[BMIM]Cl against *E. coli* and *S. aureus* with a 95% confidence level was shown in Figures 10 and 11, respectively. Based on Figure 10, the EC_{50} values of chitosan-[BMIM]Cl for *Escherichia coli* were 2.699 to 4.790 wt. %, with an EC_{50} of 3.1 wt. %. The EC_{50} values of chitosan-[BMIM]Cl for *Staphylococcus aureus* shown in Figure 11 were 2.711 to 3.700 wt. %, with an EC_{50} value of 3.2 wt. %.

The toxicity of chitosan-[BMIM]Cl mixture was ranked according to the hazard assessment scores developed by Passino and Smith (1987), who ranked toxicity to be 100-1000 mg/L as being "practically harmless," 10–100 mg/L as being "moderately toxic," 1–10 mg/L – "slightly toxic" and 0.1–1 mg/L being "highly toxic." The toxicity of chitosan-[BMIM]Cl mixture for both *E. coli* and *S. aureus* falls in the category of "relatively harmless" (EC_{50} >1000 mg/L). There were no distinct differences in the toxicity of the chitosan-[BMIM]Cl mixture despite the cell wall differences between Gram-positive and Gram-negative bacteria, which was a common phenomenon for imidazolium-based ILs (Megaw et al., 2013; Sivapragasam et al., 2019).

In the past, authors have mentioned that the toxicological effects of ILs were not due to the characteristics of bacteria cell walls but various strategies to overcome stress, such as efflux pumps, variations in the plasma membrane and enhanced production of osmolyte (Csonka, 1989; Ma et al., 2019). It was further verified by Mester et al. (2015) that these

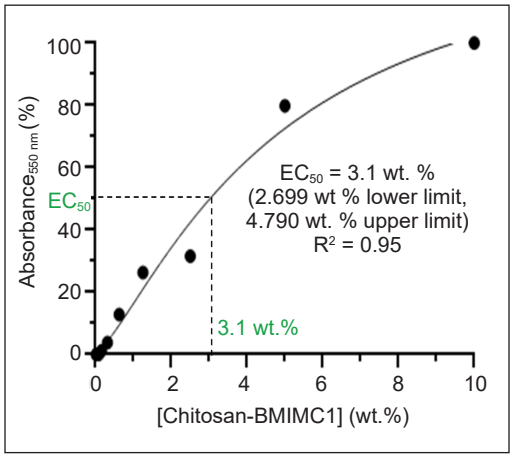

Figure 10. EC_{50} dose-response curve of chitosan-[BMIM]Cl mixture against *Escherichia coli*

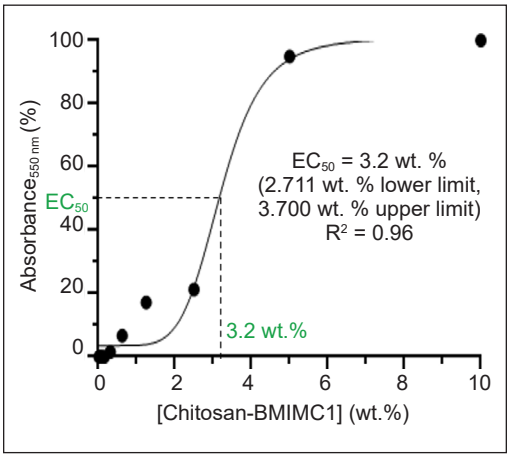

Figure 11. EC_{50} dose-response curve of chitosan-[BMIM]Cl mixture against *Staphylococcus aureus*

strategies caused huge differences in the susceptibility of bacterial strains towards the respective ILs.

The ecotoxicity of [BMIM]Cl towards *E. coli* and *S. aureus* were also studied by Ghanem et al. (2015) using the standard microbroth dilution test. The EC_{50} of [BMIM]Cl towards *E. coli* and *S. aureus* were 14409±9.9 mg/L and 12454.2±11.16 mg/L, respectively, which showed that [BMIM]Cl was "relatively harmless." Mean minimum inhibitory concentration (MIC) of [BMIM]Cl towards *E. coli* and *S. aureus* were both greater than 50000 mg/L, suggesting that it was "relatively harmless" ecologically (Weyhing-Zerrer et al., 2017).

The ecotoxicity of [BMIM]Cl has been studied using organisms from different trophic levels, such as marine bacteria, *Photobacterium phopshoreum* (Docherty, 2005), yeast, *Saccharomyces cerevisiae* (Zhu et al., 2013), duckweed, *Lemna minor* (Peric et al., 2013), Zebrafish, *Danio rerio* (Zhang et al., 2017) and human cervical carcinoma epithelial cells, HeLa cells (Stepnowski et al., 2004). Toxicity results revealed that [BMIM]Cl was "moderately toxic" to *L. minor* (48.98 mg/L), "practically harmless" to *P. phosphoreum* (898 mg/L), *S. cerevisiae* (530 mg/L) and *D. rerio* (633 mg/L) and lastly "relatively harmless" to HeLa cells.

Factors contributing to chitosan-[BMIM] Cl's toxicity were due to the structure and length of the alkyl chain on the imidazolium cation. $[BMIM]^+$ cation has a 4-carbon alkyl chain attached to the nitrogen atom in the aromatic ring. The alkyl chain and aromatic ring structure increase the hydrophobicity of [BMIM]Cl and, therefore, increases the toxicity of chitosan-[BMIM]Cl mixture towards both *Escherichia coli* and *Staphylococcus aureus* (Borkowski et al., 2016).

CONCLUSION

Chitosan (DD = 83.42%) was successfully synthesised via partial deacetylation of chitin. FTIR results of chitosan revealed the presence of free hydroxyl group and additional amino groups and reduced intensity of C=O stretch and C-H stretch, indicating the successful removal of acetyl groups from acetamide groups in chitin to form chitosan. Chitosan dissolution in [BMIM]Cl was then optimised using CCD in RSM. The optimised conditions revealed by the regression model were 130°C (X_1, temperature), 1 wt. % (X_2, initial chitosan loading), and 72 h (X_3, dissolution time). The regression model for dissolution percentage was significant ($p < 0.05$) with a non-significant lack-of-fit ($p > 0.05$). The R^2 value of the model was 0.9490 with a mean relative error of 1.78 % and RMSE of 5.0496 wt. %, indicating a good correlation between experimental and predicted values for the dissolution percentage of chitosan. No chemical changes were observed in regenerated chitosan, indicating the role of [BMIM]Cl as a direct solvent for chitosan dissolution. Lastly, the ecotoxicity of chitosan-[BMIM]Cl was evaluated

using broth microdilution assay on *Escherichia coli* and *Staphylococcus aureus*—the EC_{50} value on 10 wt. % (100,000 mg/L) chitosan-[BMIM]Cl against *E. coli* and *S. aureus* was relatively harmless, with values of 3.1 wt. % (31,000 mg/L) and 3.2 wt. % (32,000 mg/L), respectively, indicating no differences in toxicity despite cell wall variation of Gram-positive and Gram-negative bacteria.

ACKNOWLEDGMENT

This research was funded by the Ministry of Higher Education (MOHE), Malaysia, through the Fundamental Research Grant Scheme (FRGS/1/2021/STG01/QUEST/03/1). The authors thank QUEST International University, Malaysia, for the laboratory facilities and funding provided and the Centre of Research in Ionic Liquids, Universiti Teknologi PETRONAS, Malaysia, for the ILs provided.

REFERENCES

Ahing, F. A., & Wid, N. (2016). Optimization of shrimp shell waste deacetylation for chitosan production. *International Journal of Advanced and Applied Sciences*, *3*(10), 31-36. https://doi.org/10.21833/ijaas.2016.10.006

Ahyat, N. M., Mohamad, F., Ahmad, A., & Azmi, A. A. (2017). Chitin and chitosan extraction from *Portunus pelagicus*. *Malaysian Journal of Analytical Sciences*, *21*(4), 770-777. https://doi.org/10.17576/mjas-2017-2104-02

Akakuru, O. U., Louis, H., Amos, P. I., Akakuru, O., Nosike, E. I., & Ogulewe, E. F. (2018). The chemistry of chitin and chitosan justifying their nanomedical utilities. *Biochemistry & Pharmacology*, *7*, Article 1000241. https://doi.org/10.4172/2167-0501.1000241

Ali, M. H., & Abustan, I. (2014). A new novel index for evaluating model performance. *Journal of Natural Resources and Development*, *4*, 1-9. https://doi.org/10.5027/jnrd.v4i0.01

Aranaz, I., Acosta, N., Civera, C., Elorza, B., Mingo, J., Castro, C., Gandia, M. D. I. L., & Caballero, A. H. (2018). Cosmetics and cosmeceutical applications of chitin, chitosan and their derivatives. *Polymers, 10*(2), Article 213. https://doi.org/10.3390/polym10020213

Behera, S. K., Meena, H., Chakraborty, S., & Meikap, B. C. (2018). Application of response surface methodology (RSM) for optimization of leaching parameters for ash reduction from low-grade coal. *International Journal of Mining Science and Technology*, *28*, 621-629. https://doi.org/10.1016/j.ijmst.2018.04.014

Borkowski, A., Ławniczak, L., Cłapa, T., Narożna, D., Selwet, M., Pęziak, D., Markiewicz, B., & Chrzanowski, L. (2016). Different antibacterial activity of novel theophylline-based ionic liquids - Growth kinetic and cytotoxicity studies. *Ecotoxicology and Environmental Safety*, *130*, 54-64. https://doi.org/10.1016/j.ecoenv.2016.04.004

Brugnerotto, J., Lizardi, J., Goycoolea, F. M., Argüelles-Monal, W., Desbrières, J., & Rinaudo, M. (2001). An infrared investigation in relation with chitin and chitosan characterization. *Polymer*, *42*(8), 3569-3580. https://doi.org/10.1016/S0032-3861(00)00713-8

Bubalo, M., Radošević, K., Redovniković, L., Slivac, I., & Srček, V. (2017). Toxicity mechanisms of ionic liquids. *Arhiv za Higijenu Rada I Toksikologiju*, *68*(3), 171-179. https://doi.org/10.1515/aiht-2017-68-2979

Chen, Q., Xu, A., Li, Z., Wang, J., & Zhang, S. (2011). Influence of anionic structure on the dissolution of chitosan in 1-butyl-3-methylimidazolium-based ionic liquids. *Green Chemistry*, *13*(12), 3446-3452. https://doi.org/10.1039/C1GC15703E

Chowdhury, Z., Zain, S. M., Hamid, S. B. A., & Khalid, K. (2014). Catalytic role of ionic liquids for dissolution and degradation of biomacromolecules. *Bioresources*, *9*(1), 1787-1823. https://doi.org/10.15376/BIORES.9.1.1787-1823

Claros, M., Graber, T. A., Brito, I., Albanez, J., & Gavin, J. A. (2010). Synthesis and thermal properties of two new dicationic ionic liquids. *Journal of the Chilean Chemical Society*, *55*(3), 396-398. https://doi.org/10.4067/S0717-97072010000300027

Csonka, L. N. (1989). Physiological and genetic responses of bacteria to osmotic stress. *Microbiological Reviews*, *53*, 121-147. https://doi.org/10.1128/mr.53.1.121-147.1989

Czechowska-Biskup, R., Jarosińska, D., Rokita, B., Ulański, P., & Rosiak, J. (2012). Determination of degree of deacetylation of chitosan - Comparison of methods. *Progress on Chemistry and Application of Chitin and its Derivatives*, *2012*, 5-20.

da Costa Lopes, A. M., Lins, R. M. G., Rebelo, R. A., & Łukasik, R. M. (2018). Biorefinery approach for lignocellulosic biomass valorisation with acidic ionic liquid. *Green Chemistry*, *20*(17), 4043-4057. https://doi.org/10.1039/C8GC01763H

Dennis, G., Harrison, W., Agnes., K., & Erastus, G. (2016). Effect of biological control antagonists adsorbed on chitosan immobilized silica nanocomposite on *Ralstonia solanacearum* and growth of tomato seedlings. *Advances in Research*, *6*(1), 1-23. https://doi.org/10.9734/AIR/2016/22742

Docherty, K. M. (2005). Toxicity and antimicrobial activity of imidazolium and pyridinium ionic liquids. *Green Chemistry*, *7*, 185-189. https://doi.org/10.1039/B419172B

Egorova, K. S., & Ananikov, V. P. (2014). Toxicity of ionic liquids: Eco(cyto)activity as complicated, but unavoidable parameter for task-specific optimization. *Chemistry-Sustainability-Energy-Materials*, *7*(2), 336-360. https://doi.org/10.1002/cssc.201300459

El Knidri, H., El Khalfaouy, R., Laajeb, A., & Lahsini, A. (2016). Eco-friendly extraction and characterization of chitin and chitosan from the shrimp shell waste via microwave irradiation. *Process Safety and Environmental Protection*, *104*, 395-405. https://doi.org/10.1016/j.psep.2016.09.020

Elieh-Ali-Komi, D., & Hamblin, M. R. (2016). Chitin and chitosan: Production and application of versatile biomedical nanomaterials. *International Journal of Advanced Research, 4*(3), 411-427. https://pubmed.ncbi.nlm.nih.gov/27819009

Fatima, B. (2020). Quantitative analysis by IR: Determination of chitin/chitosan DD. In M. Khan (Ed.), *Modern Spectroscopic Techniques and Applications* (pp. 1-24). IntechOpen. https://doi.org/10.5772/intechopen.89708

Forsyth, S. A., MacFarlane, D. R., Thomsom, R. J., & Itzstein, M. V. (2002). Rapid, clean and mild o-acetylation of alcohols and carbohydrates in an ionic liquid. *Chemical Communications*, *7*(7), 714-715. https://doi.org/10.1039/b200306f

Ghanem, O. B., Mutalib, M. I. A., El-Harbawi, M., Gonfa, G., Chong, F. K., Alitheen, N. B. M., & Lévêque, J. M. (2015). Effect of imidazolium-based ionic liquids on bacterial growth inhibition investigated via experimental and QSAR modelling studies. *Journal of Hazardous Materials*, *297*, 198-206. https://doi.org/10.1016/j.jhazmat.2015.04.082

Gschwend, F. J. V., Chambon, C. L., Biedka, M., Brandt-Talbot, A., Fennell, P. S., & Hallett, J. P. (2019). Quantitative glucose release from softwood after pretreatment with low-cost ionic liquids. *Green Chemistry, 21*, 692-703. https://doi.org/10.1039/C8GC02155D

IEA Bioenergy. (2020). *Annual Report 2019 IEA Bioenergy*. https://www.ieabioenergy.com/wp-content/uploads/2020/05/IEA-Bioenergy-Annual-Report-2019.pdf

Islam, S., Arnold, L., & Padhye, R. (2015). Comparison and characterization of regenerated chitosan from 1-butyl-3-methylimidazolium chloride and chitosan from crab shells. *BioMed Research International*, *2015*, Article 874316. https://doi.org/10.1155/2015/874316

Kusuma, H. S., Agasi, H., & Darmokoesoemo, H. (2015). Effectiveness inhibition of fermentation legen using chitosan nanoparticles. *Journal of Molecular and Genetic Medicine*, *9*(3), Article 1000173. https://doi.org/10.4172/1747-0862.1000173

Lei, Z., Chen, B., Koo, Y. M., & MacFarlane, D. R. (2017). Introduction: Ionic liquids. *Chemical Reviews*, *117*(10), 6633-6635. https://doi.org/10.1021/acs.chemrev.7b00246

Liu, L., Wang, Y., Xie, H., Zhang, B., & Zhang, B. (2022). Enhancing the antioxidant ability of *Momordica grosvenorii* saponin to resist gastrointestinal stresses via microcapsules of sodium alginate and chitosan and its application in beverage. *Beverages*, *8*(4), Article 70. https://doi.org/10.3390/beverages8040070

Ma, Q., Gao, X., Bi, Z., Han, Q., Tu, L., Yang, Y., Shen, Y., & Wang, M. (2019). Dissolution and deacetylation of chitin in ionic liquid tetrabutylammonium hydroxide and its cascade reaction in enzyme treatment for chitin recycling. *Carbohydrate Polymers*, *230*, Article 115605. https://doi.org/10.1016/j.carbpol.2019.115605

Manzanares, P. (2020). The role of biorefining research in the development of a modern bioeconomy. *Acta Innovations*, *37*, 47-56. https://doi.org.10.32933/ActaInnovations.37.4

Matute, A. I. R., Cardelle-Cobas, A., García-Bermejo, A. B., Montilla, A., Olano, A., & Corzo, N. (2013). Synthesis, characterization and functional properties of galactosylated derivatives of chitosan through amide formation. *Food Hydrocolloids*, *33*, 245-255. https://doi.org/10.1016/j.foodhyd.2013.03.016

Megaw, J., Busetti, A., & Gilmore, B. F. (2013). Isolation and characterization of 1-alkyl-3-methylimidazolium chloride ionic liquid-tolerant and biodegrading marine bacteria. *PLoS One*, *8*(4), Article e60806. https://doi.org/10.1371/journal.pone.0060806

Mester, P., Wagner, M., & Rossmanith, P. (2015). Antimicrobial effects of short chained imidazolium-based ionic liquids - Influence of anion chaotropicity. *Ecotoxicology and Environmental Safety*, *111*, 96-101. https://doi.org/10.1016/j.ecoenv.2014.08.032

Morin-Crini, N., Lichtfouse, E., Torri, G., & Crini, G. (2019). Applications of chitosan in food, pharmaceuticals, medicine, cosmetics, agriculture, textiles, pulp and paper, biotechnology, and environmental chemistry. *Environmental Chemistry Letters, 17*, 1667-1692. https://doi.org/10.1006/s10311-019-00904-x

Naseeruteen, F., Hamid, N. S. A., Suah, F. B. M., Ngah, W. S. W., & Mehamod, F. S. (2018). Adsorption of malachite green from aqueous solution by using novel chitosan ionic liquid beads. *International Journal of Biological Macromolecules*, *107*, 1270-1277. https://doi.org/10.1016/j.ijbiomac.2017.09.111

Palpandi, C., Shanmugam, V., & Shanmugam, A. (2009). Extraction of chitin and chitosan from shell and operculum of mangrove gastropod *Nerita (Dostia) crepidularia* Lamarck. *International Journal of Medical Sciences*, *1*(5), 198-205.

Passino, D. R. M., & Smith, S. B. (1987). Acute bioassays and hazard evaluation of representative contaminants detected in great lakes fish. *Environmental Toxicology and Chemistry*, *6*(11), 901-907. https://doi.org/10.1002/etc.5620061111

Peric, B., Sierra, J., Martí, E., Cruañas, R., Garau, M. A., Arning, J., Bottin-Weber, U., & Stolte, S. (2013). (Eco)toxicity and biodegradability of selected protic and aprotic ionic liquids. *Journal of Hazardous Materials*, *261*, 99-105. https://doi.org/10.1016/j.jhazmat.2013.06.070

Poerio, A., Girardet, T., Petit, C., Eleutot, S., Jehl, J., Arab-Tehrany, E., Mano, J. F., & Cleymand, F. (2021). Comparison of the physicochemical properties of chitin extracted from *Cicada orni* sloughs harvested in three different years and characterization of the resulting chitosan. *Applied Sciences*, *11*, Article 11278. https://doi.org/10.3390/app112311278

Puspawati, N. M., & Simpen, I. N. (2010). Optimasi deasetilasi khitin dari kulit udang dan cangkang kepiting limbah restoran seafood menjadi khitosan melalui konsentrasi NaOH [Optimization of deacetylation of chitin from seafood restaurant waste shrimp skin and crab shell into chitosan through NaOH concentration]. *Jurnal Kimia*, *4*, 79-90. https://ojs.unud.ac.id/index.php/jchem/article/view/2760

Qi, L., Xu, Z., Jiang, X., Hu, C., & Zou, X. (2004). Preparation and antibacterial activity of chitosan nanoparticles. *Carbohydrate Research*, *339*(16), 2693-2700. https://doi.org/10.1016/j.carres.2004.09.007

Rahim, A. H. A., Yunus, N. M., Man, Z., Sarwono, A., Hamzah, W. S. W., & Wilfred, C. (2018). Ultrasonic assisted dissolution of bamboo biomass using ether-functionalized ionic liquid. *AIP Conference Proceedings*, *2016*, Article 020010. https://doi.org/10.1063/1.5055412

Rinaudo, M. (2006). Chitin and chitosan: Properties and application. *Progress in Polymer Science, 31*(7), 603-632. https://doi.org/10.1016/j.progpolymsci.2006.06.001

Rodríguez, H. (2021). Ionic liquids in the pretreatment of lignocellulosic biomass. *Acta Innovations*, *38*, 23-26. https://doi.org/10..32933/ActaInnovations.38.3

Roller, S., & Covill, N. (1999). The antifungal properties of chitosan in laboratory media and apple juice. *International Journal of Food Microbiology, 47*(1-2), 67-77. https://doi.org/10.1016/S0168-1605(99)00006-9

Romanazzi, G., Gabler, F. M., Margosan, D., Mackey, B. E., & Smilnick, J. L. (2009). Effect of chitosan dissolved in different acids on its ability to control postharvest gray mold of table grape. *Phytopathology*, *99*(9), 1028-1036. https://doi.org/10.1094/PHYTO-99-9-1028

Rosatella, A. A., Branco, L. C., & Afonso, C. A. M. (2009). Studies on dissolution of carbohydrates in ionic liquids and extraction from aqueous phase. *Green Chemistry*, *11*, 1406-1413. https://doi.org/10.1039/b900678h

Rumenagan, I., Suryanto, E., Modaso, R., Wullur, S., Tallei, T., & Limbong, D. (2014). Structural characteristics of chitin and chitosan isolated from the biomass of cultivated rotifer, *Brachionus rotundiformis*. *International Journal of Fisheries and Aquatic Sciences*, *3*, 12-18.

Santos, E., Rodríguez-Fernández, E., Casado-Coterillo, C., & Irabien, A. (2016). Hybrid ionic liquid-chitosan membranes for CO_2 separation: Mechanical and thermal behavior. *International Journal of Chemical Reactor Engineering*, *14*(3), 713-718. https://doi.org/10.1515/ijcre-2014-0109

Schmitz, C., Auza, L. G., Koberidze, D., Rache, S., Fischer, R., & Bortesi, L. (2019). Conversion of chitin to defined chitosan oligomers: current status and future prospects. *Marine Drugs*, *17*(8), Article 452. https://doi.org/10.3390/md17080452

Sivapragasam, M., Jaganathan, J. R., Levêque, J., Moniruzzaman, M., & Mutalib, M. I. A. (2019). Microbial biocompatibility of phosphonium- and ammonium-based ionic liquids. *Journal of Molecular Liquids*, *273*, 107-115. https://doi.org/10.1016/j.molliq.2018.10.022

Sivapragasam, M., Moniruzzaman, M., & Goto, M. (2020). An overview on the toxicological properties of ionic liquids towards microorganisms. *Biotechnology Journal*, *15*(4), Article e1900073. https://doi.org/10.1002/biot.201900073

Stepnowski, P., Składanowski, A. C., Ludwiczak, A., & Laczyńska, E. (2004). Evaluating the cytotoxicity of ionic liquids using human cell line HeLa. *Human & Experimental Toxicology*, *23*, 513-517. https://doi.org/10.1191/0960327104ht480oa

Sun, N., Rahman, M., Qin, Y., Maxim, M. L., Rodríguez, H., & Rogers, R. D. (2009). Complete dissolution and partial delignification of wood in the ionic liquid 1-ethyl-3-methylimidazolium acetate. *Green Chemistry*, *11*, 646-655. https://doi.org/10.1039/B822702K

Sun, X., Tian, Q., Xue, Z., Zhang, Y., & Mu, T. (2014). The dissolution behaviour of chitosan in acetate-based ionic liquids and their interactions: From experimental evidence to density functional theory analysis. *RSC Advances*, *4*, 30282-30291. https://doi.org/10.1039/c4ra02594f

Sun, X., Xue, Z., & Mu, T. (2014). Precipitation of chitosan from ionic liquid solution by the compressed CO_2 anti-solvent method. *Green Chemistry*, *16*, 2102-2106. https://doi.org/10.1039/C3GC42166J

Swatloski, R. P., Spear, S. K., Holbrey, J. D., & Rogers, R. D. (2002). Dissolution of cellulose with ionic liquids. *Journal of the American Chemical Society*, *124*(18), 4974-4975. https://doi.org/10.1021/ja025790m

Tamzi, N. N., Faisal, M., Sultana, T., & Ghosh, S. K. (2020). Extraction and properties evaluation of chitin and chitosan prepared from different crustacean waste. *Bangladesh Journal of Veterinary and Animal Sciences, 8*(2), 69-76.

Tan, H. T., & Lee, K. (2012). Understanding the impact of ionic liquid pretreatment on biomass and enzymatic hydrolysis. *Chemical Engineering Journal*, *183*, 448-458. https://doi.org/10.1016/j.cej.2011.12.086

Thomas, P. A., & Marvey, B. B. (2016). Room temperature ionic liquids as green solvent alternatives in the metathesis of oleochemical feedstocks. *Molecules*, *21*(2), Article 184. https://doi.org/10.3390/molecules21020184

Wang, W. T., Zhu, J., Wang, X. L., Huang, Y., & Wang, Y. Z. (2010). Dissolution behavior of chitin in ionic liquids. *Journal of Macromolecular Science, Part B*, *49*(3), 528-541. https://doi.org/10.1080/00222341003595634

Wang, X., Li, H., Cao, Y., & Tang, Q. (2011). Cellulose extraction from wood chip in an ionic liquid 1-allyl-3-methylimidazolium chloride (AmimCl). *Bioresource Technology*, *102*, 7959-7965. https://doi.org/10.1016/j.biortech.2011.05.064

Weyhing-Zerrer, N., Gundolf, T., Kalb, R., Oßmer, R., Rossmanith, P., & Mester, P. (2017). Predictability of ionic liquid toxicity from a SAR study on different systematic levels of pathogenic bacteria. *Ecotoxicology and Environmental Safety*, *139*, 394-403. https://doi.org/10.1016/j/ecoenv.2017.01.055

Wu, J., Zhang, J., Zhang, H., He, J., Ren, Q., & Guo, M. (2004). Homogenous acetylation of cellulose in a new ionic liquid. *Biomacromolecules*, *5*(2), 266-268. https://doi.org/10.1021/bm034398d

Wu, Y., Sasaki, T., Irie, S., & Sakurai, K. (2008). A novel biomass-ionic liquid platform for the utilization of native chitin. *Polymer, 49*, 2321-2327. https://doi.org/10.1016/j.polymer.2008.03.027

Xie, H., Zhang, S., & Li, S. (2006). Chitin and chitosan dissolved in ionic liquids as reversible sorbents of CO_2. *Green Chemistry, 8*(7), 630-633. https://doi.org/10.1039/B517297G

Xu, B., Li, Q., Zhuang, L., Wang, Q., Li, C., Wang, G., Xie, F., & Halley, P. J. (2016). Dissolution and regeneration behavior of chitosan in 3-methyl-1-(ethylacetyl)imidazolium chloride. *Fibers and Polymer*, *17*(11), 1741-1748. https://doi.org/10.1007/s12221-016-6747-6

Yang, X., Qian, C., Li, Y., & Li, T. (2016). Dissolution and resourcfulization of biopolymers in ionic liquids. *Reactive and Functional Polymers*, *100*, 181-190. https://doi.org/10.1016/j.reactfunctpolym.2016.01.017

Zakrzewska, M. E., Bogel-Łukasik, E., & Bogel-Łukasik, R. (2010). Solubility of carbohydrates in ionic liquids. *Energy Fuels*, *24*, 737-745. https://doi.org/10.1021/ef901215m

Zhang, C., Shao, Y., Zhu, L., Wang, J., Wang, J., & Guo Y. (2017). Acute toxicity, biochemical toxicity and genotoxicity caused by 1-butyl-3-methylimidazolium chloride and 1-butyl-3-methylimidazolium tetrafluoroborate in zebrafish (*Danio rerio*) livers. *Environmental Toxicology and Pharmacology*, *51*, 131-137. https://doi.org.10.1016/j-etap.2017.02.018

Zhang, H., Wu, J., Zhang, J., & He., J. (2005). 1-allyl-3-methylimidazolium chloride room temperature ionic liquid: A new and powerful nonderivatizing solvent for cellulose. *Macromolecules*, *38*(20), 8272-8277. https://doi.org/10.1021/ma0505676

Zhang, M., Zhang, F., Li, C., An, H., Wan, T., & Zhang, P. (2022). Application of chitosan and its derivative polymers in clinical medicine and agriculture. *Polymers*, *14*, Article 958. https://doi.org/10.3390/polym14050958

Zhang, Y., Liu, Y, Chu, Z., Shi, L., & Jin, W. (2013). Amperometric glucose biosensor based on direct assembly of prussian blue film with ionic liquid-chitosan matrix assisted enzyme immobilization. *Sensors and Actuators B: Chemical*, *176*, 978-984. https://doi.org/10.1016/j.snb.2012.09.080

Zhao, D., Yu, S., Sun, B., Gao, S., Guo, S., & Zhao, K. (2018). Biomedical applications of chitosan and its derivative nanoparticles. *Polymers, 10*(4), Article 462. https://doi.org/10.3390/polym10040462

Zhu, S., Yu, P., Lei, M., Tong, Y., Zheng, L., Zhang, R., Ji, J., Chen, Q., & Wu, Y. (2013). Investigation of the toxicity of the ionic liquid 1-butyl-3-methylimidazolium chloride to *Saccharomyces cerevisiae* AY93161 for lignocellulosic ethanol production. *Polish Journal of Chemical Technology*, *15*(2), 94-98. https://doi.org/10.2478/pjct-2013-0029

Zhuang, L., Zhong, F., Qin, M., Sun, Y., Tan, X., Zhang, H., Kong, M., Hu, K., & Wang, G. (2020). Theoretical and experimental studies of ionic liquid-urea mixtures on chitosan dissolution: Effect of cationic structure. *Journal of Molecular Liquids*, *317*, Article 113918. https://doi.org/10.1016/j.molliq.2020.113918